

Spin-Orbit Coupling and Anomalous Angular-Dependent Magnetoresistance in the Quantum Transport Regime of PbS

Kazuma Eto, A. A. Taskin, Kouji Segawa, and Yoichi Ando

Institute of Scientific and Industrial Research, Osaka University, Ibaraki, Osaka 567-0047, Japan

We measured magnetotransport properties of PbS single crystals which exhibit the quantum linear magnetoresistance (MR) as well as the static skin effect that creates a surface layer of additional conductivity. The Shubnikov-de Haas oscillations in the longitudinal MR signify the peculiar role of spin-orbit coupling. In the angular-dependent MR, sharp peaks are observed when the magnetic field is slightly inclined from the longitudinal configuration, which is totally unexpected for a system with nearly spherical Fermi surface and points to an intricate interplay between the spin-orbit coupling and the conducting surface layer in the quantum transport regime.

PACS numbers: 72.20.My, 71.18.+y, 73.25.+i, 75.47.-m

Recently, non-trivial consequences of the spin-orbit coupling (SOC) in crystalline solids are a major theme in condensed matter physics [1]. For example, the spin Hall effect is a striking manifestation of the SOC in non-magnetic materials [2], and the SOC in non-centrosymmetric superconductors gives rise to an unconventional order-parameter symmetry [3]. Even more strikingly, it was recognized that a certain class of narrow-gap semiconductors where the energy gap is a product of the SOC are topological insulators, whose valence band structures is characterized by a non-trivial Z_2 topological invariant [4–9]. The three-dimensional topological insulators host helically spin-polarized surface states and are predicted to exhibit various novel phenomena [7–11]. After the discovery of the topological-insulator nature in $\text{Bi}_{1-x}\text{Sb}_x$, Bi_2Se_3 , and Bi_2Te_3 [12–15], those three materials are under intense investigations.

In this context, the narrow-gap semiconductor PbS would make a useful comparison, because its energy gap is due to a strong SOC but its valence band structure lends itself to the trivial Z_2 topological class [8]; namely, PbS is a non-topological insulator. Nevertheless, this material may be called an “incipient” spin Hall insulator, since the energy gap of the SOC origin in PbS causes a large Berry phase in the Bloch states and leads to a finite intrinsic spin Hall conductivity σ_H^s even in the insulating state [16]. Therefore, the role of the SOC in the transport properties of this material is worth investigating with the modern understanding.

PbS has a rock salt crystal structure and has a direct energy gap of about 0.3 eV located at the four equivalent L points of the Brillouin zone [17]. Depending on whether S is excessive or deficient, both p - and n -type PbS can be prepared, and in both cases the Fermi surface (FS) is very nearly spherical [17, 18]. This material was well studied in the past for its potential in the infrared applications [17]. More recently, PbS is attracting attentions in the photovoltaic community because of the multi-exiton generation [19]. In this Letter, we report our detailed study of the magnetoresistance (MR)

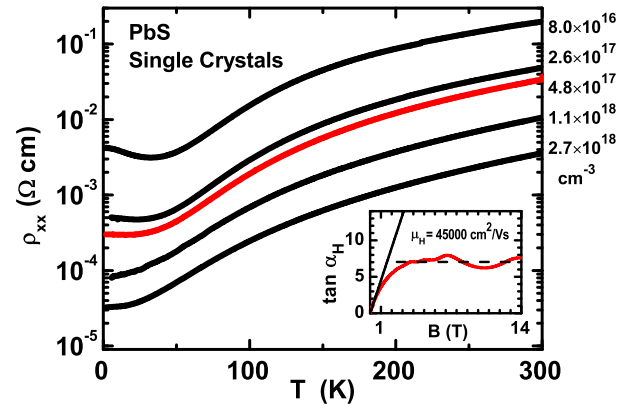


FIG. 1: (Color online) Temperature dependence of ρ_{xx} for a series of p -type PbS single crystals, whose n_h is indicated on the right. Inset shows $\tan \alpha_H$ vs B for the $4.8 \times 10^{17} \text{ cm}^{-3}$ sample, which exhibits a deviation from the classical linear behavior (shown by the solid straight line) and a saturation above 4 T in the quantum transport regime; the low-field slope is equal to μ_H and gives $4.5 \times 10^4 \text{ cm}^2/\text{Vs}$.

in low-carrier-density PbS, focusing on its angular dependence. To our surprise, we observed sharp peaks in the angular-dependent MR in high magnetic fields, which is totally unexpected for a three-dimensional (3D) material with a small spherical FS. Although the exact mechanism of this anomalous behavior is not clear at the moment, our data points to an important role of the SOC in the quantum transport regime. In addition, the formation of a surface layer with additional conductivity due to skipping orbits (called “static skin effect” [20]) appears to be also playing a role in the observed angular dependence. The unexpected angular-dependent MR points to a hitherto-overlooked effect that could become important in the magnetotransport properties of narrow-gap semiconductors with a strong SOC.

High-quality single crystals of PbS were grown by a vapor transport method from a stoichiometric mixture of 99.998% purity Pb and 99.99% purity S. The mixture was sealed in an evacuated quartz tube and was reacted

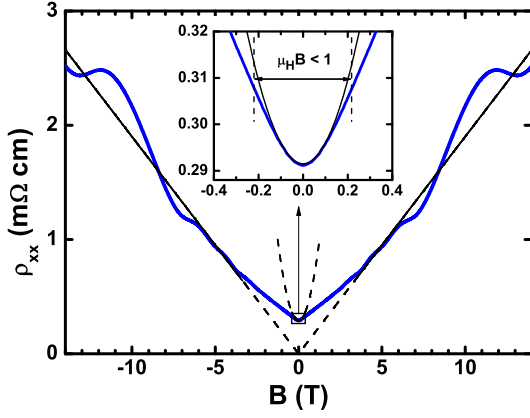


FIG. 2: (Color online) Transverse MR at 1.5 K with B along [001]. The straight lines are the background linear MR, on top of which pronounced SdH oscillations are superimposed. Inset shows the B^2 dependence observed in the low-field classical regime ($\mu_H B < 1$) and its fitting (thin solid line).

for 5 – 10 h at 980°C. After the reaction, the resulting material was vaporized and transported to the other end of the sealed tube by making a large temperature difference, which worked as a purification stage. The obtained polycrystals were taken out and again sealed in a new evacuated quartz tube for the crystal growth stage: The polycrystal-containing end of the tube was kept at 850°C, and sublimed PbS was transported to the other end kept at 840°C for one week. The obtained single crystals were annealed in sulfur vapor to tune the type and the density of carriers, during which the crystal temperature and the sulfur vapor pressure were controlled independently. We have prepared a series of samples with various carrier density as shown in Fig. 1. In the following we focus on a p -type sample with the carrier density n_h of $4.8 \times 10^{17} \text{ cm}^{-3}$, which was obtained by annealing the crystal at 533°C with the sulfur vapor source kept at 90°C.

The resistivity ρ_{xx} and the Hall resistivity ρ_{yx} were measured simultaneously by using a standard six-probe method on a thin rectangular sample whose top and bottom surfaces were cleaved (001) plane. The current I was always along the [100] direction. The Shubnikov-de Haas (SdH) oscillations were measured by sweeping the magnetic field B between +14 and -14 T for a series of field directions. Continuous rotations of the sample in constant magnetic fields were used for measuring the angular dependence of the MR, in which the direction of the magnetic field B was either [001] \rightarrow [010] (transverse geometry) or [001] \rightarrow [100] (transverse to longitudinal geometry).

Figure 2 shows the transverse MR measured at 1.5 K with B along [001]. Pronounced SdH oscillations are clearly seen, and one may notice that the background MR does not show the ordinary B^2 dependence. This is because the range of the weak-field regime ($\mu_H B <$

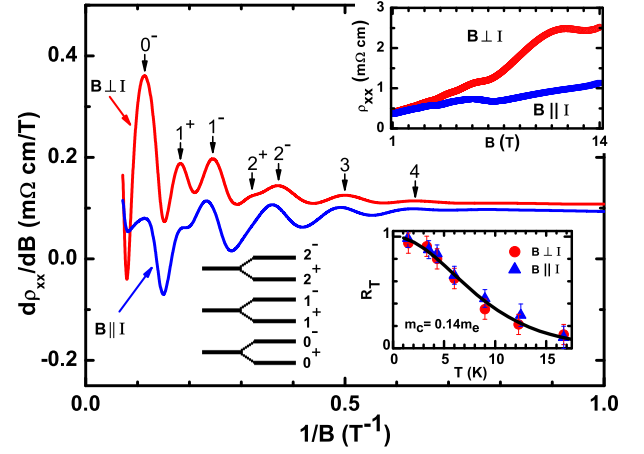


FIG. 3: (Color online) SdH oscillations in the transverse ($B \perp I$) and longitudinal ($B \parallel I$) MR at 1.5 K. Upper inset shows the raw data, and the main panel presents $d\rho_{xx}/dB$ vs $1/B$. In the “ $B \parallel I$ ” measurement, the magnetic field was 8° off from the exactly parallel direction. Lower left inset shows the schematic Landau level diagram. Lower right inset shows the temperature dependence of the normalized SdH amplitude, which yields $m_c = 0.14m_e$ (m_e is the free electron mass).

1), where the B^2 dependence is observed, is extremely narrow in our sample, as shown in the inset of Fig. 2 (μ_H is the Hall mobility). It is worth noting that our sample shows a nearly- B -linear background MR in the strong-field regime ($\mu_H B > 1$), rather than a tendency to saturation which is usually observed in metals. This high-field behavior is the so-called “quantum linear MR” proposed by Abrikosov [21]. Such a behavior is expected in the quantum transport regime where the condition $n_h < (eB/\hbar c)^{2/3}$ is satisfied [21], and in our sample this regime is realized for $B > 4$ T. In this sense, our PbS presents a straightforward realization of the quantum linear MR and is different from $\text{Ag}_{2+\delta}\text{Se}$ or $\text{Ag}_{2+\delta}\text{Te}$ where the linear MR is observed down to very low field [21].

The SdH oscillations measured in the transverse ($B \perp I$) and longitudinal ($B \parallel I$) MR are presented in Fig. 3 by plotting $d\rho_{xx}/dB$ vs $1/B$. One can see that we are resolving the spin-splitting of the Landau levels in high magnetic fields and that the crossing of the 0^- state by the Fermi level is observed (see the lower left inset of Fig. 3 for the Landau level diagram); this means that all the electrons are in the 0^+ state in the highest field (14 T) and hence the system is in the quantum limit. Also, one may notice that the amplitude of some particular peaks, 0^- , 1^+ , and 2^+ , are significantly diminished in the longitudinal configuration ($B \parallel I$) compared to the transverse one where all the peaks are well developed. Such a behavior was previously observed in $\text{Hg}_{1-x}\text{Cd}_x\text{Te}$ [22] and in $\text{Pb}_{1-x}\text{Sn}_x\text{Te}$ [23], and was elucidated to be due to some selection rules [22] imposed by the SOC which prohibits scattering between certain Landau sublevels in the longitudinal configuration. Besides this peculiar dif-

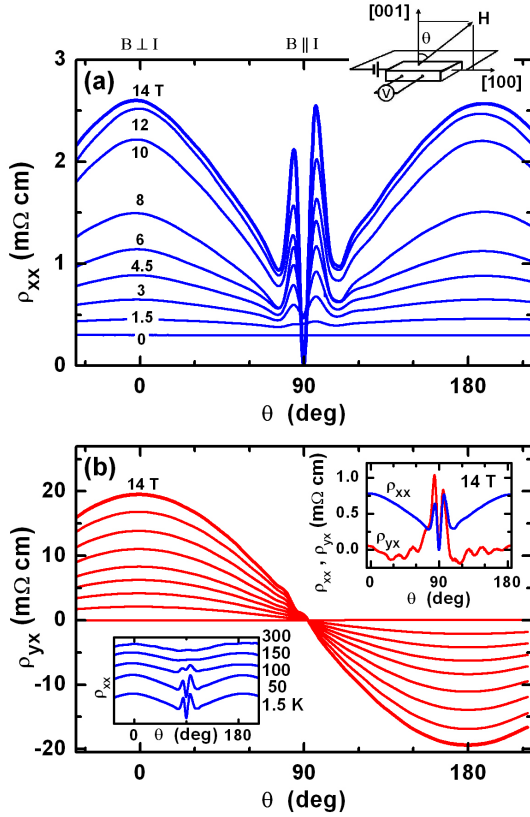


FIG. 4: (Color online) Angular-dependence of (a) ρ_{xx} and (b) ρ_{yx} for the transverse-to-longitudinal rotation (top inset shows the geometry). In panel (b), the upper inset compares the deviation of $\rho_{yx}(\theta)$ from the $\cos\theta$ dependence to $\rho_{xx}(\theta)$ multiplied by 0.3, while the lower inset shows how the anomalous peaks weaken with temperature (data are vertically shifted for clarity).

ference, the peak positions are almost the same for the two field directions, which is because the FS in PbS is nearly spherical [17, 18]. Also, the cyclotron mass m_c extracted from the temperature dependence of the SdH amplitude (lower right inset) using the Lifshitz-Kosevich formula [24] is identical for the two directions.

The carrier density n_h calculated from the FS volume seen by the SdH oscillations is $4.8 \times 10^{17} \text{ cm}^{-3}$, which agrees well with the value of $n_h = 4.6 \times 10^{17} \text{ cm}^{-3}$ obtained from the high-field Hall coefficient $R_{H\infty}$. It is worth noting that the Hall mobility μ_H calculated from $R_{H\infty}$ and ρ_{xx} at 0 T is $4.5 \times 10^4 \text{ cm}^2/\text{Vs}$, while the mobility μ_{SdH} obtained from the SdH oscillations is only $3.8 \times 10^3 \text{ cm}^2/\text{Vs}$ [25]. This discrepancy is essentially due to the fact that ρ_{xx} and the Dingle temperature T_D (smearing factor in the SdH effect [24]) are determined by different scattering processes; namely, ρ_{xx} is primarily determined by the backward scattering, while T_D is sensitive to both forward and backward scattering [24, 26]. Apparently, only small-angle scatterings are relevant in high-mobility PbS, which leads to the 12 times difference

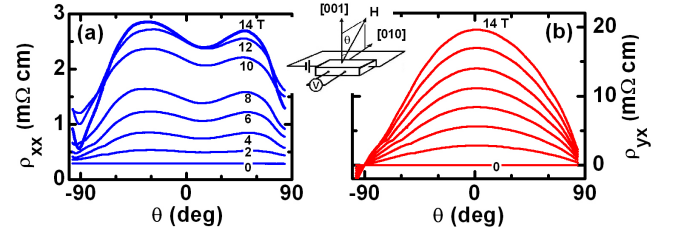


FIG. 5: (Color online) Angular-dependence of (a) ρ_{xx} and (b) ρ_{yx} for the transverse rotation (inset shows the geometry). The ρ_{xx} data shown here are after removing the admixture of the ρ_{yx} component in the ρ_{xx} measurement.

between μ_H and μ_{SdH} .

Now let us present the most surprising result. The angular-dependent MR for the transverse-to-longitudinal rotation (I was along [100] and B was rotated from [001] toward [100]) is shown in Fig. 4(a), and the corresponding angular dependence of ρ_{yx} is shown in Fig. 4(b) (the magnetic-field angle θ is measured from [001]). In Fig. 4(a), pronounced peaks are observed when θ is near 90° , that is, when the magnetic field is slightly inclined from the longitudinal configuration. The θ dependence of ρ_{yx} also shows a feature near 90° , which can be more easily seen in the upper inset of Fig. 4(b) where the deviation of the measured $\rho_{yx}(\theta)$ from a smooth $\cos\theta$ dependence is plotted together with the $\rho_{xx}(\theta)$ data (which is multiplied by 0.3). One can easily see in this inset that the sharp peak occurs in both ρ_{xx} and ρ_{yx} at the same θ ; in addition, $\rho_{yx}(\theta)$ apparently shows periodic oscillations in a wide range of θ , whose relation to the sharp peak is not obvious. In any case, given that the FS in PbS is nearly spherical and that they cannot give rise to any open orbit, such a sharp peak in the angular-dependent MR is totally unexpected.

To gain insight into the origin of the unexpected peak in $\rho_{xx}(\theta)$, the angular-dependent MR data in a different rotation plane is useful. Figure 5 shows such data for the transverse rotation (I was along [100] and B was rotated from [001] toward [010]). As one can see in Fig. 5, there is no sharp peak in this configuration, which immediately indicates that the unexpected peaks are peculiar to the near-longitudinal configuration. Besides the absence of the sharp peaks, there is a notable feature in Fig. 5: Since PbS has a cubic symmetry, the MR for $\theta = 0^\circ$ (B along [001]) and 90° (B along [010]) should be the same, since [001] and [010] are crystallographically identical and the measurement configuration is both transverse. However, the actual data in Fig. 5 indicates that they are different, which suggests that there must be some additional factor which affects the resistivity in magnetic field. In the past, similar anisotropy was observed in clean specimens of low-carrier-density materials such as Bi [27] and Sb [28], and was explained in terms of the static skin effect [20], that is, the formation of a surface layer of additional

conductivity due to skipping orbits when the magnetic field is nearly parallel to a specular surface. In this regard, since the top and bottom surfaces of our sample were cleaved (001) plane, it is understandable that the static skin effect creates a surface conduction layer near the specular (001) surface for the magnetic field along [010], leading to a reduced resistivity.

An additional factor to consider regarding the MR anisotropy in the present case is the SOC which diminishes some of the peaks in the SdH oscillations for $B \parallel I$. In fact, as one can infer in the upper inset of Fig. 3, the change in the SdH oscillations due to the SOC is partly responsible for the difference in MR between $B \perp I$ and $B \parallel I$. Another factor to consider is the crossover between classical and quantum transport regimes: As we already discussed, the quantum regime is arrived above 4 T in the transverse configuration. (This crossover can also be seen in the B dependence of $\tan \alpha_H$, which is linear in B in the classical regime but saturates in the quantum regime [29], see Fig. 1 inset.) On the other hand, in the longitudinal configuration, the electron motion along the current direction is *not* quantized, and therefore ρ_{xx} for $B \parallel I$ is always “classical”. This means that in our measurement in high magnetic fields, there is a crossover from the classical to the quantum regime when the configuration changes from longitudinal to transverse. Since the MR behavior is different in the two regimes, this crossover must be partly responsible for the observed MR anisotropy.

Although we have not been able to elucidate the mechanism for the sharp peaks in the angular-dependent MR shown in Fig. 4(a), we can see that there are three factors that are likely to participate in this phenomenon: (i) the SOC which diminishes some of the peaks in the SdH oscillations for $B \parallel I$, (ii) the static skin effect which creates a conducting surface layer, and (iii) the crossover between classical and quantum transport regimes. It is useful to note that the sharp peaks weaken only gradually with increasing temperature and are still observable at 100 K [lower inset of Fig. 4(b)], while the SdH oscillations disappear above ~ 20 K (lower right inset of Fig. 3); this suggests that the sharp peak is not directly related to quantum oscillations. We also note that the SOC is expected to affect not only the SdH oscillations but also the static skin effect when the magnetic field is inclined from the surface, because in such a configuration the surface reflection of an electrons necessarily involves a transition to a different Landau level [20], and the same selection rules imposed by the SOC as those in the SdH case [22] would apply. We expect that the anomalous angular-dependent MR is a result of an intricate interplay between the above three factors.

In conclusion, we have observed sharp peaks in the angular-dependent MR in PbS when the magnetic field is slightly inclined from the longitudinal ($B \parallel I$) configuration, which is totally unexpected for a low-carrier-density

system with nearly spherical Fermi surface. While the mechanism of this peak is to be elucidated in future, we show that the spin-orbit coupling, the static skin effect, and the crossover between classical and quantum transport regimes, are all important in the magnetotransport properties of PbS. This unusual phenomenon would help establish a general understanding of the magnetotransport in narrow-gap semiconductors with a strong SOC, which is important in elucidating the transport properties of topological insulators.

This work was supported by JSPS (KAKENHI 19340078 and 2003004) and AFOSR (AOARD-08-4099). We thank H. D. Drew and V. Yakovenko for discussions.

-
- [1] N. Nagaosa, J. Phys. Soc. Jpn. **77**, 031010 (2008).
 - [2] S. Murakami, Adv. in Solid State Phys. **45**, 197 (2005).
 - [3] S. Fujimoto, J. Phys. Soc. Jpn. **76**, 051008 (2007).
 - [4] C. L. Kane and E. J. Mele, Phys. Rev. Lett. **95**, 146802 (2005).
 - [5] B. A. Bernevig, T. L. Hughes, and S.-C. Zhang, Science **314**, 1757 (2006).
 - [6] J. E. Moore and L. Balents, Phys. Rev. B **75**, 121306(R) (2007).
 - [7] L. Fu, C. L. Kane, and E. J. Mele, Phys. Rev. Lett. **98**, 106803 (2007).
 - [8] L. Fu and C. L. Kane, Phys. Rev. B **76**, 045302 (2007).
 - [9] X.-L. Qi, T. L. Hughes, and S.-C. Zhang, Phys. Rev. B **78**, 195424 (2008).
 - [10] L. Fu and C. L. Kane, Phys. Rev. Lett. **100**, 096407 (2008).
 - [11] X.-L. Qi, R. Li, J. Zang, and S.-C. Zhang, Science **323**, 1184 (2009).
 - [12] D. Hsieh *et al.*, Nature **452**, 970 (2008).
 - [13] H.-J. Zhang *et al.*, Nat. Phys. **5**, 438 (2009).
 - [14] Y. Xia *et al.*, Nat. Phys. **5**, 398 (2009).
 - [15] Y. L. Chen *et al.*, Science **325**, 178 (2009).
 - [16] S. Murakami, N. Nagaosa, and S.-C. Zhang, Phys. Rev. Lett. **93**, 156804 (2004).
 - [17] R. Dalven, Infrared Phys. **9**, 141 (1969).
 - [18] P. J. Stiles, E. Burstein, and D. N. Langenberg, J. Appl. Phys. **32**, 2174 (1961).
 - [19] J. J. H. Pijpers *et al.*, Nat. Phys. **5**, 811 (2009).
 - [20] V. G. Peschanskii and M. Y. Azbel', Soviet Phys. JETP **28**, 1045 (1969).
 - [21] A. A. Abrikosov, J. Phys. A: Math. Gen. **36**, 9119 (2003).
 - [22] K. Suizu and S. Narita, Phys. Lett. A **43**, 353 (1973).
 - [23] S. Narita and Y. Takafuji, Solid State Commun. **20**, 357 (1976).
 - [24] D. Shoenberg, *Magnetic Oscillations in Metals* (Cambridge University Press, 1984).
 - [25] Analysis of the SdH data yields $T_D = 4$ K, which gives the scattering time 3×10^{-13} s. Using $m_c = 0.14m_e$, we obtain $\mu_{\text{SdH}} = 3.8 \times 10^3$ cm²/Vs. The observed SdH frequency of 7.7 T corresponds to $k_F = 1.53 \times 10^6$ cm⁻¹, which gives $E_F = 6.4$ meV, $v_F = 1.26 \times 10^7$ cm/s, and $\ell_{\text{SdH}} = 3.8 \times 10^{-6}$ cm. This is contrasted to the transport mean free path $\ell_{\text{tr}} = 4.5 \times 10^{-5}$ cm.
 - [26] S. Das Sarma and F. Stern, Phys. Rev. B **32**, 8442 (1985).
 - [27] Y. A. Bogod, V. V. Eremenko, and L. K. Chubova, Soviet

- Phys. JETP **29**, 17 (1969).
- [28] Y. A. Bogod and V. B. Krasovitskii, Soviet Phys. JETP **36**, 544 (1973).
- [29] In the quantum regime, both ρ_{xx} and ρ_{yx} becomes linear in B , leading to a constant $\tan \alpha_H$.